Technical Paper for *Nuclear Technology*

Title: An Approach for Validating Actinide and Fission Product Burnup Credit Criticality Safety Analyses – Criticality (k_{eff}) Predictions

Authors: J. M. Scaglione, D. E. Mueller, and J. C. Wagner

Affiliation: Reactor and Nuclear Systems Division
Oak Ridge National Laboratory
P.O. Box 2008, Bldg. 5700
Oak Ridge, Tennessee 37831-6170

Corresponding Author: John M. Scaglione
(865) 574-9284
(865) 574-3527 fax
scaglionejm@ornl.gov

Text pages: 24
Figures: 6
Tables: 6

Abstract:

One of the most significant remaining challenges associated with expanded implementation of burnup credit in the United States is the validation of depletion and criticality calculations used in the safety evaluation—in particular, the availability and use of applicable measured data to support validation, especially for fission products. Applicants and regulatory reviewers have been constrained by both a scarcity of data and a lack of clear technical basis or approach for use of the data. U.S. Nuclear Regulatory Commission (NRC) staff have noted that the rationale for restricting their Interim Staff Guidance on burnup credit (ISG-8) to actinide only has been based largely on the lack of clear, definitive experiments that can be used to estimate the bias and uncertainty for computational analyses associated with using burnup credit. To address the issue of validation, the NRC initiated a project with the Oak Ridge National Laboratory to (1) develop and establish a technically sound validation approach (both depletion and criticality) for commercial spent nuclear fuel (SNF) criticality safety evaluations based on best-available data and methods and (2) apply the approach for representative SNF storage and transport configurations/conditions to demonstrate its usage and applicability, as well as to provide reference bias results. The purpose of this paper is to describe the criticality (k_{eff}) validation approach and resulting observations and recommendations. Validation of the isotopic composition (depletion) calculations is addressed in a companion paper. For criticality validation, the approach is to utilize (1) available laboratory critical experiment (LCE) data from the International Handbook of Evaluated Criticality Safety Benchmark Experiments *and the French Haut Taux de Combustion program to support validation of the principal actinides and (2) calculated sensitivities, nuclear data uncertainties, and the limited available fission product LCE data to predict and verify individual biases for relevant minor actinides and fission products. This paper (1) provides a detailed description of the approach and its technical bases, (2) describes the application of the approach for representative pressurized water reactor and boiling water reactor safety analysis models, and (3) provides reference bias results based on the prerelease SCALE 6.1 code package and ENDF/B-VII nuclear cross-section data.*

Keywords: criticality, burnup, validation, spent nuclear fuel

I. INTRODUCTION

Criticality safety analyses in the United States are performed to show that a proposed fuel storage or transport configuration meets the applicable requirements of Title 10 of the *Code of Federal Regulations* Parts 50, 52, 70, 71, and 72 [1]. For fuel storage at nuclear power plants, criticality analyses include calculations that are performed to demonstrate that the proposed configuration will meet the maximum neutron multiplication (k_{eff}) limits specified in the applicable requirements and guidance. As the fuel is used in the reactor, the ^{235}U content decreases and concentrations of fission products (FPs) and other actinides increase. Hence, some criticality analyses take credit for the reduction in reactivity of nuclear fuel that results from its use in the reactor. Such credit is referred to as burnup credit (BUC).

Consistent with applicable industry standards (i.e., ANSI/ANS-8 [2]) and regulatory guidance [3, 4], criticality safety evaluations require validation of the calculational method with critical experiments that are as similar as possible to the safety analysis models and for which the k_{eff} values are known. This poses a challenge for validation of BUC criticality analyses as critical experiments with both actinide and FP nuclides similar to spent nuclear fuel (SNF) are not available. As a result, validation for spent fuel pools (SFPs) relies on critical experiments without FPs [5] supplemented with margin to cover poor validation of actinides and fission products. Burnup credit for transportation has frequently been limited to actinide-only spent fuel compositions consistent with ISG-8, Rev. 2 [6]. Credit for FPs is needed for high-density SNF storage in SFPs and beneficial for enabling acceptance of the majority of discharged SNF assemblies in high-capacity casks [7]. Therefore, a physics-based, defensible approach to establishing a bounding estimate for bias in k_{eff} prediction using uncertainties in nuclear data for cases in which critical-experiment data are lacking or nonexistent has been explored. The results of this study serve as the basis for recommendation 4 in ISG-8, Rev. 3 [4]. A more comprehensive presentation of work presented in this paper is available in NUREG/CR-7109 [8], which is available from the U.S. Nuclear Regulatory Commission (NRC).

The computational method is the combination of the computer code, the data used by the computer code, and the calculational options selected by the user. For k_{eff} calculations, the nuclear data used includes errors associated with data measurement, evaluation, and representation in forms usable by computer programs. As a result, calculated results frequently do not exhibit exact agreement with expectations. Hence, the goal of validation is to establish a predictable relationship between calculated results and reality. Typically, the results of a validation study include the difference or "bias" between calculated and expected results and the uncertainty in this bias.

Calculation of an accurate computational bias, one that accurately reflects the difference between the calculated and actual k_{eff} values for a safety analysis model, requires use of critical experiments that are similar to the safety analysis model. The critical experiments need to use the nuclear data in a similar energy-dependent manner. Even if the same materials are present in an experiment and in the safety analysis model, local variation in the energy-dependent neutron spectrum could cause different energy ranges of the nuclear data to be exercised, resulting in an incorrect bias. Hence, it is not enough to simply have the same materials in both the experiments and the safety analysis model, which hereafter is referred to as the application or application model.

The generally accepted guidance for critical-experiment selection is that the critical experiments should be as similar to the application model as is practical. Historically, similarity has been left largely to the professional judgment of the engineers performing and reviewing the work. Unfortunately, a high degree of similarity occurs only in cases where critical experiments were designed to simulate the real operational situation. This is particularly true for validation of BUC application models, for which there are no laboratory critical experiments (LCEs) that include enriched uranium, plutonium, other actinides, and FPs in the same proportions as those contained in commercial spent fuel.

The traditional approach to criticality validation is to compute bias and bias uncertainty values through the use of trending analyses. For a traditional trending analysis, a suite of critical-experiment benchmarks are selected that have characteristics similar to corresponding values in the application for which the subcritical limit is to be established. Some characteristics used to evaluate system similarity include fissile element(s), fissile concentration/enrichment, moderator type, geometrical configuration, hydrogen-to-fissile atom ratios (H/X), and energy of average neutron lethargy causing fission (EALF). Typically the trending parameters are calculated as averages over the entire benchmark experiment. Each of the experiments in the benchmark suite is modeled with the same code and data that will be used in the criticality-safety analysis of the application. The difference between the expected and calculated values of the effective neutron multiplication factor, k_{eff}, of a critical experiment is considered to be the computational bias for that experiment. The expected computational bias of the application system is established through a trending analysis of the bias for all of the selected critical experiments as a function of their characteristics (e.g., H/X, EALF). The uncertainty in the bias is established through a statistical analysis of the trend. NUREG/CR-6698, *Guide for Validation of Nuclear Criticality Safety Calculational Methodology* [9], provides guidance that may be useful for trending analysis. For the results presented in this paper, the USLSTATS [10, 11] computer code was used for trending analyses.

II. CALCULATION OF BIAS AND BIAS UNCERTAINTY

The calculations and results presented in this paper were generated using a quality-assurance-controlled prerelease version of SCALE 6.1 with ENDF/B-VII cross-section libraries. All depletion calculations for the application models were performed using either the TRITON [12, Sect. T01] t-depl sequence or the STARBUCS [12, Sect. C10] sequence. Both sequences use the ORIGEN-S [12, Sect. F07] program to calculate burned fuel compositions. In SCALE 6.1 the nuclear decay data are derived from ENDF/B-VII.0 (hereafter referred to as ENDF/B-VII), including the half-lives, branching fractions, and recoverable energy per disintegration. Decay branching fractions are included for the following decay modes: beta, electron capture and positron emission, isomeric transition, alpha, spontaneous fission, delayed neutron (β^-,n) emission, and double β^- decay. Cross-section data are developed from the JEFF 3.0/A activation files and ENDF/B-VII cross sections for nuclides present in the transport calculation. Criticality calculations were performed with the CSAS5 [12, Sect. C05] or CSAS6 [12, Sect. C06] sequences and the ENDF/B-VII 238-energy group library. CSAS5 and CSAS6 use the KENO V.a and KENO VI Monte Carlo transport codes, respectively.

II.A. Representative Safety Analysis Models

To provide a basis for comparison and to demonstrate the overall approach, several representative safety analysis models or application models were developed simulating a pressurized water reactor (PWR) SFP configuration, a generic PWR cask configuration, and a boiling water reactor (BWR) SFP configuration. Although different PWR spent fuel composition nuclide sets have been evaluated, the results in this paper correspond to all nuclides available in the SCALE code [12]. The generic cask application models used a 5 year cooling period, as is typical for spent fuel storage cask evaluations, flooded with full-density unborated water and a target k_{eff} of 0.94. The PWR SFP application models used a 3 day post-irradiation decay period, with unborated water and a target k_{eff} of 0.99. The BWR SFP application model used burned fuel compositions from standard cold core geometry (SCCG) peak reactivity, after a 3 day post-irradiation decay period, in an infinite spent storage rack model with unborated water and a target k_{eff} of 0.94.

II.A.1. PWR Application Description

The PWR fuel storage rack is represented as a laterally infinite array of loaded fuel storage cells reflected on the top and bottom by 30 cm of full-density water. Each storage cell is a stainless steel box having an internal dimension of 22.352 cm (8.8 in.) and a wall thickness of 0.292 cm (0.115 in.). One 0.203-cm-thick (0.080-in.-thick) Boral® plate with a 0.020 g $^{10}B/cm^2$ loading is modeled between each storage cell. The center-to-center spacing for this model is 23.139 cm (9.110 in.). The Westinghouse 17 × 17 optimized fuel assembly (OFA) design is modeled as centered in the storage cell. Only the 365.76 cm (12 ft) of active fuel length of the assembly is modeled. The poison panels are also modeled to the same axial length. To evaluate the potential for variation in biases as a function of burnup, the work presented in this paper shows biases and bias uncertainties for application models at 10 and 40 GWd/MTU. An illustration of a spent fuel pool and representative spent fuel assembly model are provided in Figure 1.

A generic cask model with a 32 PWR assembly capacity, referred to as the GBC-32 and described in NUREG/CR-6747 [13], was previously developed to serve as a computational benchmark. The Westinghouse 17 × 17 OFA fuel assembly design is used in this model as well. The features of the GBC-32 model include 32 cells with 365.76-cm-tall and 19.05-cm-wide Boral® (0.0225 g $^{10}B/cm^2$) panels between and on the external faces of each cell. The cells have inner dimensions of 22 × 22 cm and are spaced on 23.76 cm centers. The cell walls are constructed of stainless steel. The cells sit 15 cm above the bottom of a stainless steel cask having an inner radius of 87.5 cm and internal height of 410.76 cm. The radial thickness of the side walls is 20 cm, and the cask bottom and lid are 30 cm thick. Similar to what is being done for the SFP analysis to evaluate the potential for variation in biases as a function of burnup, the results presented in this paper show biases and bias uncertainties for the application models at 10 and 40 GWd/MTU. An illustration of a representative spent fuel cask and spent fuel assembly are provided in Figure 1.

Table I shows some key parameters for the application models. The final uranium enrichment and plutonium fraction vary axially due to the use of axial burnup profiles. Two averages are presented for these parameters. One is the simple average from each of the 18 axial zones. The second uses the axial fission density fraction as a weighting factor, thus giving increased weight to the axial zones having the most impact on system neutron multiplication. For bias and bias uncertainty determination, use of the fission density weighted values is more appropriate.

II.A.2. BWR Application Description

Modern BWR fuel assemblies are designed with several features different from those present in PWR assemblies. BWR fuel assembly differences include large central water rod regions, radially and axially varying initial ^{235}U enrichments, as well as part-length fuel rods, and also typically include fuel rods in which Gd_2O_3 is mixed with the UO_2 in the fuel pellets. The gadolinium is a strong thermal neutron absorber that burns out relatively quickly (during the first cycle of irradiation), but is present in BWR assemblies in sufficient quantity to typically result in a reactivity rise to a peak value at assembly average burnup values below 20 GWd/MTU. Since reactivity initially increases with burnup, using the fresh fuel bundle in the fuel storage analysis would not be conservative. Consequently, criticality analyses for BWR fuel storage are usually performed with fuel at the maximum or "peak" reactivity point.

The number of fuel rods with Gd_2O_3 and the weight fraction of the Gd_2O_3 in these rods may vary. Because of the many assembly lattice variations, BWR criticality analyses characterize each lattice, depleted in hot reactor conditions, according to its maximum two-dimensional k_∞ in cold conditions in reactor geometry. After the peak k_∞ in SCCG is identified, the burned fuel compositions from the peak k_∞ burnup are typically decayed for 3 days, to allow xenon decay, and then used in a fuel assembly in a fuel storage rack model to establish the relationship between peak SCCG k_∞ and the k_{eff} for the fuel in the fuel storage rack model. This relationship identifies the maximum SCCG k_∞ that will result in a fuel storage rack k_{eff} that meets the regulatory requirement.

The BWR SFP application model consists of a representative 10 × 10 assembly of 5 wt % ^{235}U fuel rods burned to about 11 GWd/MTU. The assembly included eight Gd_2O_3(3 wt %)+UO_2 fuel rods and two water rods that displaced eight fuel rods. The Gd_2O_3+UO_2 rods are modeled using five equal-volume radial regions to accurately model the gadolinium depletion. The assembly is stored in a 0.2-cm-thick Zircaloy fuel channel having an inner dimension of 12.95 cm. Each fuel storage rack cell is modeled as a square tube of steel that is 0.18 cm thick and has an inner dimension of 14.75 cm. A single B_4C+Al plate is placed between each storage cell. Each neutron-absorbing plate is 0.203 cm thick, 11.64 cm wide, and has a neutron absorber loading of 0.020 g ^{10}B/cm^2. The model has reflected boundary conditions on all sides and is effectively infinite in all directions. The initial enrichment, number of gadolinium rods, gadolinium rod enrichment, and storage cell pitch were selected such that when the fuel is depleted to peak reactivity, the fuel storage rack model has a calculated k_{eff} value of 0.94. The EALF for the BWR application model is 0.456 eV. The burned fuel fission-density-weighted average composition included uranium with a ^{235}U enrichment of 3.82 wt % and a plutonium-to-uranium ratio of 0.331 wt % Pu.

II.B. Critical Experiments

A total of 609 critical experiments were considered in the initial set to be used for validation, including 124 low enriched uranium (LEU) and 194 mixed uranium and plutonium critical configurations from the *International Handbook of Evaluated Criticality Safety Benchmark Experiments* (IHECSBE) [14]. The critical configurations used are from the following IHECSBE evaluations:

- LEU-COMP-THERM-001, 002, 010, 017, 022, 023, 024, 026, 042, 050, and 079
- LEU-MISC-THERM-005
- LEU-SOL-THERM-002, 003, and 004
- MIXED-COMP-THERM-001, 002, 003, 004, 005, 006, 007, 008, 009, 011, and 012
- MIXED-SOL-THERM-001, 002, 004, and 005

The validation set also included 156 configurations from the French Haut Taux de Combustion (HTC) experiment set that includes uranium and plutonium nuclides in appropriate proportions relevant to spent fuel similar to a fuel assembly with an initial enrichment of 4.5 wt % ^{235}U and burned to 37.5 GWd/MTU [15]. The HTC experiment data were published in a series of four reports by the French Institut de Radioprotection et de Sûreté Nucléaire (IRSN) [16, 17, 18, 19] and are considered commercial proprietary property. There are currently some restrictions on who may use the data and for what purposes.

The validation set also included 135 configurations from the French Fission Product Program experiments [20, 21, 22, 23, 24, 25]. From 1998 to 2004, a series of critical experiments referred to as the FP experimental program was conducted by the IRSN at the experimental criticality facility in Valduc, France. The experiments focused on the worth of seven FP nuclides (either singly or as nuclide mixtures in various experiments): ^{103}Rh, ^{133}Cs, ^{143}Nd, ^{145}Nd, ^{149}Sm, ^{152}Sm, and ^{155}Gd. In all experiments with FPs, the FP test material was in the form of slightly acidic solutions. Three experimental phases (FP Phases 1–3) were performed, each distinguished by the manner in which the FP solutions were configured relative to the fuel rods. The majority of the configurations used LEU dioxide fuel rods, but some also mixed in fuel from the HTC experiment set. The FP critical experiment descriptions are commercial proprietary and are not expected to be released for applicant use. Therefore, their use in this paper is for demonstrating the relative merits of analytical techniques that can be used to address FP validation gaps when applicable FP experiments are unavailable.

II.C. Critical Benchmark Experiment Selection

II.C.1. Traditional Critical-Experiment Selection

Historically, when critical experiments could not be created to simulate specific applications, analysts typically used qualitative and integral quantitative comparisons to select critical experiments. Qualitative parameters considered might include fissionable, moderating, and neutron-absorbing materials present; type of geometry (i.e., fuel pin lattices); type of neutron reflection (i.e., bare, water reflected, steel reflected, etc.); and qualitative characterization of the energy dependence of the neutron flux as thermal, intermediate, or fast. Quantitative parameters have included average neutron energy group of neutrons causing fission, EALF, ratio of moderating nuclei to fissile nuclei, fuel enrichment, soluble boron concentration, lattice fuel pin pitch, etc. Experienced analysts would use these techniques and professional judgment to select critical experiments for use in computational method validation. Using this method, one may select all experiments listed in Section II.B; hence, 474 experiments from the IHECSBE and HTC experiment sets (the 135 FP critical experiments are not expected to be available for applicant use) are used to develop the bias and bias uncertainty based on conventional analysis techniques below.

II.C.2. Sensitivity/Uncertainty-Based Critical-Experiment Selection

A method utilizing sensitivity and uncertainty (S/U) analysis techniques to assess similarity of one model to another is available in the SCALE computer code. The SCALE computer code includes calculational sequences (i.e., TSUNAMI-1D, -2D, and -3D) that can be used to calculate the sensitivity of the k_{eff} value of a system to variation of the nuclear data used in the k_{eff} calculation. Sensitivities can be calculated as a function of mixture, location, nuclide, nuclear reaction, and neutron energy group using first-order linear perturbation theory [12, Sect. F22] that utilizes the angular- and energy-dependent neutron flux solutions from forward and adjoint transport calculations. As calculated by TSUNAMI, sensitivity is the fractional change in k_{eff} due to a fractional change in a nuclear data value or $S \equiv (\Delta k/k)/(\Delta\sigma/\sigma)$. A sensitivity of +1.0 means a 1.0% increase in the value of the nuclear data will result in a 1.0% increase in the system k_{eff} value.

A technique implemented in the SCALE S/U tools can be used to perform detailed comparisons of application and critical experiment models. The technique compares the detailed sensitivity data for the two systems, giving greater weight to comparisons of sensitivities for nuclides and reactions with higher nuclear data uncertainties. Specifically, for each model, TSUNAMI-IP [12, Sect. M18.1] combines the sensitivity data and the cross-section covariance data to generate nuclide-, reaction-, and energy-dependent k_{eff} uncertainty data. A correlation coefficient, identified as the c_k value, is calculated indicating the degree to which each application and critical experiment model pair shares k_{eff} uncertainty. A high c_k value, approaching one, indicates that the two compared systems share a similar sensitivity to the same higher uncertainty nuclear data. Based on the assumption that computational biases are due primarily to nuclear data errors and that the nuclear data uncertainty values should indicate the potential for such nuclear data errors, two highly correlated systems should exhibit the same computational bias.

Oak Ridge National Laboratory (ORNL) experience with the SCALE S/U tools has indicated that a critical experiment is adequately similar to an application model if the c_k value is no lower than 0.9. Critical experiments with c_k values between 0.8 and 0.9 are considered only marginally similar, and use of experiments with c_k values below 0.8 is not recommended. Table II presents the similarity assessment results indicating the number of experiments calculated to be within a given c_k range.

A more detailed evaluation of the similarity assessment results indicated the following: only HTC experiments generated c_k values in excess of 0.9; IHECSBE evaluations MIX-COMP-THERM-002 through -009 and -012 generated some c_k values between 0.8 and 0.9; and IHECSBE evaluations MIX-COMP-THERM-001 and -011 and MIX-SOL-THERM-001, -002, -004, and -005 generated some c_k values in the 0.7 to 0.8 range and could be considered as potential candidates for other BUC application models. Note the lack of experiments with c_k values as high as 0.8 for the BWR SFP model suggests that further study is needed to identify appropriate benchmarks.

II.D. Validation of the Principal Actinides

The USLSTATS computer program was used to determine the bias and bias uncertainty for the application models as a function of various trend parameters using the LEU, the mixed uranium-plutonium, and the HTC mixed oxide fuel (MOX) LCEs. Results are presented based on traditional critical benchmark selection techniques as well as using S/U analysis tools for applicable critical experiment selection. Trending analysis results are presented for EALF, final uranium enrichment, and final plutonium fraction. In addition, for the S/U analysis benchmark selection results, bias, and bias uncertainty are also calculated as a function of the similarity index (c_k). No bias and bias uncertainty results are presented for the BWR application model using the S/U analysis benchmark selection process because none of the critical experiments had a c_k value of at least 0.8 when compared to the BWR application model.

In the tables that follow, “bias” is calculated as calculated k_{eff} minus expected k_{eff}. Thus a positive bias would imply the calculated values were higher than the expected values. Positive bias values are generally not credited in criticality safety analyses. The “fit uncertainty” is the one-standard-deviation uncertainty in the bias resulting from application of the linear least-squares fitting technique to the critical experiment results. The “total uncertainty" includes the necessary additional uncertainty that would be added to the bias value to yield a 95% probability and 95% confidence level. Table III presents the results based on traditional critical experiment selection techniques where all 474 experiments were used in the trending analysis, and Table IV presents the results when S/U analysis techniques are used to select applicable critical experiments. The "none" shown for bias and bias uncertainty for the final enrichment trend and the plutonium content trend means that the value of the trend parameter for the application model was outside the range of parameter values for the critical experiments.

The bias and bias uncertainty values presented in Table III and Table IV are based on a critical experiment range of applicability that only accounts for the actinide isotopes: ^{234}U, ^{235}U, ^{236}U, ^{238}U, ^{238}Pu, ^{239}Pu, ^{240}Pu, ^{241}Pu, ^{242}Pu, and ^{241}Am plus some FP isotopes (i.e., ^{149}Sm, ^{103}Rh, ^{133}Cs, ^{nat}Sm, and ^{nat}Eu). The range of applicability in Table IV is different from Table III due to the use of different benchmark experiments. As can be seen in Tables III and IV, the calculated bias and bias uncertainty values can vary significantly with burnup, with the parameter used in the trending analysis, and the set of critical experiments used. For example, the bias and bias uncertainty calculated using the traditional method yields similar results across application models, depending on trending parameter, because the same set of benchmarks is used. When the benchmark experiments are selected using application-model-specific parameters, the results vary considerably across the applications models, hence demonstrating the sensitivity to the set of critical experiment benchmarks used for validation.

II.E. Validation of the Minor Actinides and Fission Products

Spent nuclear fuel includes nuclides for which there are few or no appropriate critical experiments available. Historically, when an analyst could not validate a particular material in a safety analysis model, the analyst typically either removed the material or used a Δk penalty or uncertainty selected using engineering judgment. In this section, a validation approach to address nuclides in the material compositions for which there are few or no applicable critical experiments, namely the minor actinides and FPs, is presented. The approach is based on the uncertainty in k_{eff} due to nuclear data uncertainties.

All nuclear data used in criticality calculations have some error. The amount of error varies with the type of data, the experimental apparatus and procedure used to measure the data, the quality and amount of measured data, nuclear models used to fill in data gaps, the evaluation technique used to combine measured and modeled data and resolve conflicting data, and conversion of the data into formats suitable for use in the computational method. Detailed or "high-fidelity" covariance data are available for only a limited number of nuclides. A collaborative effort involving nuclear data experts from Brookhaven National Laboratory (BNL), Los Alamos National Laboratory (LANL), and ORNL have developed approximate or "low-fidelity" covariance data for nearly all other nuclides and reactions of interest. The SCALE 44-group covariance data file is composed of a combination of high- and low-fidelity nuclear data uncertainties. This information is in the form of variance and covariance information, where covariance is the degree to which different data and their uncertainties are related to each other. Model-specific sensitivity data, which are in units of $(\Delta k/k)/(\Delta\sigma/\sigma)$, can be used to translate nuclear data uncertainties, which are in units of $\Delta\sigma/\sigma$, into uncertainty in the model k_{eff} value.

The SCALE sensitivity and uncertainty analysis tools calculate the uncertainty in k_{eff} due to nuclear data uncertainties, creating a way to quantify potential k_{eff} bias associated with errors in the nuclear data. The matrix algebra used to calculate the k_{eff} uncertainty is provided in Section F22.2.6 of the SCALE 6.1 manual [12]. Figures 2 through 5 present the individual calculated biases for the four groups of LCEs described and used in this paper along with the uncertainty in k_{eff} due to nuclear data for each experiment. Ignoring the contribution of experimental uncertainty to the bias and thereby assuming the bias is due entirely to nuclear data errors, one would expect that around 67% of the individual critical experiment biases would be within one standard deviation of the nuclear data uncertainty. Note that Figure 2 shows 98% of the calculated bias values for the 124 LEU experiments are within one standard deviation of the uncertainty in k_{eff} due to nuclear data uncertainty. This suggests that the nuclear data uncertainties are overestimated. From Figures 3, 4, and 5, respectively, 71% of the 194 Pu+U LCE bias values were within one standard deviation, 98% of the 156 HTC LCE bias values were within one standard deviation, and 100% of the 135 Fission Product Programme critical-experiment bias values were within one standard deviation. Note that the Pu+U LCE have several clusters of data points (e.g., experiment number 130 to 158) outside the nuclear data uncertainty band. The calculated results are consistent with the benchmark results provided by the evaluators [14], suggesting inconsistencies within the experiment descriptions, and not the nuclear data. Averaging all of the experiment sets shows that 90% of the experiment biases fall within one standard deviation of the expected value. This comparison provides confidence that the uncertainty in k_{eff} due to nuclear data uncertainties can be used to provide bounding estimates of the actual bias values.

When calculating bias and bias uncertainty for a specific application, because each applicable critical experiment uses the same nuclear data set, there is a significant source of common or systematic error. The impact of the systematic error is best quantified using the average or trended bias as calculated above. The variability around the average bias reflects the variability in the critical experiment systems and the accuracy to which they have been described, and does not reflect the ability of the computational method to accurately calculate k_{eff} for a safety analysis model. To provide an estimate of the additional penalty for crediting other nuclides where little or no validation data are available, the uncertainty in k_{eff} due to nuclear data uncertainties can be used for the additional nuclides. Prior to the use of detailed uncertainty analysis techniques, additional margin was adopted to cover potential biases associated with unvalidated nuclides and features. The amount of margin was typically based on engineering judgment and/or perturbation studies. Frequently, it was necessary to adopt a larger margin because values did not have adequate quantitative basis.

The SCALE TSUNAMI-IP module was used to combine the model-specific k_{eff} sensitivity data with the nuclear data uncertainty information in the SCALE cross-section covariance data file to translate the nuclear data uncertainties into detailed k_{eff} uncertainty information for each application model. The process is described in more detail in Section F22.2.5 of Reference 12. Note that the uncertainty calculation incorporates correlations in uncertainties between energy groups, between reactions, and, in some cases, between nuclides. The k_{eff} uncertainty (1σ) results for each of the application models are presented in Table V.

Comparison of the bias values from Tables III and IV with the total uncertainty value for “All nuclides” in Table V shows that the bias values calculated using statistical analysis of the critical experiment results are all within one standard deviation of the total uncertainty in k_{eff} due to nuclear data uncertainty. This suggests that, consistent with the study presented, the uncertainty in k_{eff} due to nuclear data uncertainties could be used to conservatively estimate biases associated with the computational method, including biases associated with nuclear data errors. A comparison of the k_{eff} uncertainty for “All nuclides” with the uncertainty associated with only major actinides in Table V indicates that the uncertainty associated with the major actinides contributes nearly all of the uncertainty in k_{eff}. Hence, validation of the major actinides is most important. The next highest contributor to the overall uncertainty is the category of structural materials. The results also indicate that the bias in k_{eff} due to FP nuclear data errors is small in comparison with the bias due to nuclear data errors for the actinides. A plot of k_{eff} uncertainty as a function of burnup for the SFP application model is shown in Figure 6 to illustrate these effects.

II.F. Fission Product Bias and Bias Uncertainty

To substantiate the premise that computational biases are caused primarily by errors in the nuclear data (as discussed in Section II.E), which are quantified and bounded with a 1σ confidence by the cross-section covariance data, the available FP critical-experiment data were evaluated using traditional validation techniques.

Care must be taken in the use of the FP biases calculated from the experiments to determine an appropriate bias to apply to the application model. It may not be appropriate to apply a bias calculated for a FP using experiments which include only that FP or include it in a system that is rather different from the application, to the application model. The amount of the FP and neutron energy spectrum shifts as well as the presence of other FPs and other materials may significantly affect the bias associated with the FP of interest.

The overall bias is typically calculated using a single-sided lower tolerance limit established such that there is a 95% confidence that at least 95% of the population is above the limit. One possible method to account for the FPs in the application model would be to subtract the individual FP biases from the computational bias developed using the non-FP experiments when the bias is negative. However, because the bias is developed on a 95% probability/95% confidence interval, the individual FP biases would need to be similarly developed, resulting in very high penalties as a result of the low FP critical-experiment sample sizes that require high tolerance factors to provide biases at the 95% probability/95% confidence level.

An alternative means for incorporating the FP biases into the application model is to adjust the individual FP biases from each experiment using their respective k_{eff} sensitivities, as illustrated in Eq. (1). Sensitivity adjustment is more appropriate than using FP worth weighting because some experiments could be saturated with the FP material, thus becoming less sensitive to the associated nuclear data errors, and result in nonconservative adjustments.

The sensitivities can be estimated using direct perturbation calculations, wherein the analyst manually varies the amount of the FP in the model, or with the SCALE code system.

$$\beta_{FP} = \sum_i \frac{S_i^{app}}{S_i^{exp}} \times \beta_i \ , \tag{0}$$

where

β_{FP} = total FP bias for the application,

i = individual FP for which critical experiment data exist,

S_i^{app} = sensitivity of FP isotope (i) in application model,

S_i^{exp} = sensitivity of FP isotope (i) in critical experiment, and

β_i = individual FP isotope bias taken as difference between expected value and calculated value.

Biases were calculated for the individual FPs using FP LCE data for the following nuclides (either individually or as nuclide mixtures): ^{103}Rh, ^{133}Cs, ^{nat}Nd (^{143}Nd +^{145}Nd), ^{149}Sm, ^{152}Sm, and ^{155}Gd. The best-estimate bias for an individual experiment was calculated by taking the difference between the expected calculated k_{eff} value with no FPs as determined from the trending analysis equations and the calculated value for the experiment with FPs. The sensitivity-adjusted bias and uncertainty for the individual FPs for the PWR SFP application model are presented in Table VI. The bias is the average from the different individual FP experiments, and the total uncertainty represents the appropriately combined fit uncertainty and calculational uncertainty. The nuclear data uncertainty is provided in the second column for comparison with the fission product bias and bias uncertainties.

As can be seen, the bias fluctuates with trending parameter, but the uncertainty remains about the same for each nuclide and is consistent with or exceeds the calculated FP bias. Due to the large total uncertainty component, a direct comparison of the calculated FP biases with the FP nuclear data uncertainties does not definitely support or refute the use of nuclear data uncertainty to bound the bias, but it does show that the bias values are generally of the same order of magnitude and that the bias values predicted with the experimental data are subsumed within the uncertainty band, hence supporting the premise that nuclear data uncertainty can be used to bound the bias for unvalidated nuclides. Use of additional critical-experiment data with FPs may significantly reduce the bias uncertainty and thus provide more useful bias and bias uncertainty estimates to draw definitive conclusions.

III. CONCLUSIONS

This paper presented a validation approach for commercial SNF BUC criticality safety evaluations based on best-available data and methods, and applied the approach for representative SNF storage and transport configurations/conditions to demonstrate its usage and applicability, as well as to provide reference bias results. Generic safety application models representative of PWR and BWR fuel storage racks and PWR fuel in a high-capacity transportation cask were used for the demonstration.

The results show that sufficient critical-experiment data exist to adequately validate k_{eff} calculations via conventional validation approaches for the primary actinides. Therefore, the bias in k_{eff} calculations due to the primary actinide compositions can be determined based on applicable critical experiments, such as the HTC critical-experiment data and other MOX critical experiments. Recommended candidates for mixed U-Pu systems from the IHECSBE are provided in Section II.C.2. Use of the HTC and recommended IHECSBE mixed U-Pu LCEs should provide adequate validation for uranium, plutonium, and ^{241}Am.

For actinide and FP nuclides for which adequate critical experimental data are not available, an approach based on calculated sensitivities and nuclear data uncertainties was demonstrated for generating conservative estimates of bias. These conservative estimates for bias were generated using the sensitivity and uncertainty analysis tools and nuclear data uncertainty file available in SCALE. The uncertainty analysis technique yields an application-specific value for the uncertainty in k_{eff} due to the uncertainty in the nuclear data. Although direct confirmation of the conservatism in using nuclear data uncertainties to estimate FP biases was not definitively demonstrated due to the large uncertainties in bias values calculated based on the limited available FP experiment data, the comparisons do not invalidate this approach. Other comparisons for cases where adequate critical-experiment data are available, and hence definitive conclusions can be made, have demonstrated the validity and conservatism of the proposed approach.

Additional details concerning this study and its conclusions and recommendations are available in report NUREG/CR-7109 [8], which is available from the NRC.

IV. ACKNOWLEDGMENTS

The work presented in this paper was performed under contract with the NRC Office of Nuclear Regulatory Research (RES). The authors thank D. Algama, the NRC Project Manager; M. Aissa and R. Y. Lee of RES; K. A. Wood of the Office of Nuclear Reactor Regulation (NRR); A. B. Barto of the Office of Nuclear Material Safety and Safeguards (NMSS); and C. N. Van Wert of the Office of New Reactors (NRO) for their support and guidance. Many valuable review comments were received from NRC staff members of RES, NRR, NMSS, and NRO. The authors also wish to thank H. Turpin for assistance in formatting and preparation of the final paper.

REFERENCES

1. *Code of Federal Regulations,* Title 10, "Energy."

2. "Burnup Credit for LWR Fuel," ANSI/ANS-8.27-2008, an American National Standard, published by the American Nuclear Society, LaGrange Park, IL (2008).

3. NRC Information Notice 2011-03: Nonconservative Criticality Safety Analyses for Fuel Storage, U.S. Nuclear Regulatory Commission, February 16, 2011.

4. Spent Fuel Project Office, *Interim Staff Guidance – 8, rev. 3, Burnup Credit in the Criticality Safety Analyses of PWR Spent Fuel in Transport and Storage Casks, ISG-8, rev. 3*, U.S. Nuclear Regulatory Commission, September 26, 2012.

5. Letter from L. Kopp to T. Collins, "Guidance on the Regulatory Requirements for Criticality Analysis of Fuel Storage at Light-Water Reactor Power Plants," U.S. Nuclear Regulatory Commission, August 19, 1998.

6. Spent Fuel Project Office, *Interim Staff Guidance – 8, rev. 2, Burnup Credit in the Criticality Safety Analyses of PWR Spent Fuel in Transport and Storage Casks, ISG-8, rev. 2*, U.S. Nuclear Regulatory Commission, September 27, 2002.

7. C. V. Parks, J. C. Wagner, D. E. Mueller, and I. C. Gauld, "Full Burnup Credit in Transport and Storage Casks—Benefits and Implementation," *Radwaste Solutions* **14**(2), 32–41, March/April 2007.

8. J. M. Scaglione, D. E. Mueller, J. C. Wagner, and W. J. Marshall, *An Approach for Validating Actinide and Fission Product Burnup Credit Criticality Safety Analyses – Criticality (k_{eff}) Predictions*, NUREG/CR-7109 (ORNL/TM-2011/514), prepared for the U.S. Nuclear Regulatory Commission by Oak Ridge National Laboratory, Oak Ridge, TN, April 2012.

9. J. C. Dean, R. W. Tayloe, Jr., and D. Morey, *Guide for Validation of Nuclear Criticality Safety Calculational Methodology*, NUREG/CR-6698, prepared for the U.S. Nuclear

Regulatory Commission by Science Applications International Corporation, January 2001.

10. V. R. Cain, *A Computer Code to Perform Analyses of Criticality Validation Results*, Y/DD-574, Martin Marietta Energy Systems, Inc., Oak Ridge Y-12 Plant, Oak Ridge, TN, September 1995.

11. J. J. Lichtenwalter, S. M. Bowman, M. D. DeHart, and C. M. Hopper, *Criticality Benchmark Guide for Light-Water-Reactor Fuel in Transportation and Storage Packages*, NUREG/CR-6361 (ORNL/TM-13211), prepared for the U.S. Nuclear Regulatory Commission by Oak Ridge National Laboratory, Oak Ridge, TN, March 1997.

12. *SCALE: A Comprehensive Modeling and Simulation Suite for Nuclear Safety Analysis and Design*, ORNL/TM-2005/39, Version 6.1, Oak Ridge National Laboratory, Oak Ridge, TN, June 2011. Available from Radiation Safety Information Computational Center at Oak Ridge National Laboratory as CCC-785.

13. J. C. Wagner, *Computational Benchmark for Estimation of Reactivity Margin from Fission Products and Minor Actinides in PWR Burnup Credit*, NUREG/CR-6747 (ORNL/TM-2000/306), prepared for the U.S. Nuclear Regulatory Commission by Oak Ridge National Laboratory, Oak Ridge, TN, October 2001.

14. *International Handbook of Evaluated Criticality Safety Benchmark Experiments*, NEA/NSC/DOC(95)03, NEA Nuclear Science Committee, September 2009.

15. D. E. Mueller, K. R. Elam, and P. B. Fox, *Evaluation of the French Haut Taux de Combustion (HTC) Critical Experiment Data*, NUREG/CR-6979 (ORNL/TM-2007/83), prepared for the U.S. Nuclear Regulatory Commission by Oak Ridge National Laboratory, Oak Ridge, TN, September 2008.

16. F. Fernex, *Programme HTC – Phase 1: Réseaux de Crayons dans l'Eau Pure (Water-Moderated and Reflected Simple Arrays) Reevaluation des Expériences*, DSU/SEC/T/2005-33/D.R, Valduc, France, IRSN (2006). PROPRIETARY document.

17. F. Fernex, *Programme HTC – Phase 2: Réseaux Simples en Eau Empoisonnée (Bore et Gadolinium) (Reflected Simple Arrays Moderated by Poisoned Water with Gadolinium or Boron) Réévaluation des Experiences*, DSU/SEC/T/2005-38/D.R, Valduc, France, IRSN (2006). PROPRIETARY document.

18. F. Fernex, *Programme HTC – Phase 3: Configurations "Stockage en Piscine" (Pool Storage) Réévaluation des Experiences*, DSU/SEC/T/2005-37/D.R, Valduc, France, IRSN (2006). PROPRIETARY document.

19. F. Fernex, *Programme HTC – Phase 4: Configurations "Châteaux de Transport" (Shipping Cask) Réévaluation des Experiences*, DSU/SEC/T/2005-36/D.R., Valduc, France, IRSN (2006). PROPRIETARY document.

20. N. Leclaire, T. Ivanova, E. Létang, E. Girault, and J. Thro, "Fission Product Experimental Program: Validation and Computational Analysis," *Nucl. Sci. Eng*. **161**, 188–215 (2009).

21. N. Leclaire, "Fission Products Experimental Programme Exploitation, 1st Part, Analysis of the Fission Products Experimental Programme: Physical Type Experiments Related to the Validation of 6 FP Absorption Cross Sections (^{103}Rh, ^{133}Cs, ^{143}Nd, ^{149}Sm, ^{152}Sm, ^{155}Gd) in Slightly Acidic Solutions," DSU/SEC/T/2009-173/D.R., Index A, Institut de Radioprotection et de Sûreté Nucléaire (2009). PROPRIETARY document.

22. N. Leclaire, "Fission Products Experimental Programme Exploitation, 2nd Part, 'Elementary Dissolution' Type Criticality Experiments: PWR Rods Arrays in Slightly Acidic Solutions Poisoned or Not by Fission Products," DSU/SEC/T/2009-174/D.R.,

Index A, Institut de Radioprotection et de Sûreté Nucléaire (2009). PROPRIETARY document.

23. N. Leclaire, "Fission Products Experimental Programme Exploitation, 2nd Part, 'Elementary Dissolution' Type Criticality Experiments: PWR Rods Arrays Immersed in Depleted Uranyl Nitrate Solutions Poisoned or Not by Fission Products," DSU/SEC/T/2009-175/D.R., Index A, Institut de Radioprotection et de Sûreté Nucléaire (2009). PROPRIETARY document.
24. N. Leclaire, "Fission Products Experimental Programme Exploitation, 3rd Part, 'Dissolution in a Large Non-adjusted Tank' Type Criticality Experiments on an Array of UO_2 Rods, Immersed in Depleted Uranyl Nitrate Solutions," DSU/SEC/T/2009-176/D.R., Index A, Institut de Radioprotection et de Sûreté Nucléaire (2009). PROPRIETARY document.
25. N. Leclaire, "Fission Products Experimental Programme Exploitation, 3rd Part, 'Advanced Dissolution' Type Criticality Experiments: Arrays of HBU Rods in Depleted Uranyl Nitrate Solutions Poisoned or Not by Fission Products," DSU/SEC/T/2009-177/D.R., Index A, Institut de Radioprotection et de Sûreté Nucléaire (2009). PROPRIETARY document.

Table I. PWR application characteristics

Model	Burnup (GWd/MTU)	EALF (eV)	Simple average		Fission density weighted average	
			Final enr. (wt % ^{235}U)	Pu/(U+Pu) (wt % Pu)	Final enr. (wt % ^{235}U)	Pu/(U+Pu) (wt % Pu)
PWR SFP	10	0.202	1.735	0.562	1.956	0.427
PWR SFP	40	0.295	1.995	1.298	2.227	1.212
GBC-32	10	0.201	1.540	0.570	1.780	0.416
GBC-32	40	0.295	1.815	1.267	2.150	1.144

Table II. Similarity assessment summary

Model	Burnup (GWd/MTU)	$c_k < 0.8$	$0.8 \leq c_k < 0.9$	$0.9 \leq c_k$
PWR SFP	10	355	119	0
PWR SFP	40	250	128	96
GBC-32	10	318	152	4
GBC-32	40	197	122	155
BWR SFP	11	474	0	0

Table III. Bias and bias uncertainty results using traditional method

Application model	Initial enrichment (wt % ^{235}U)	Final BU (GWd/MTU)	EALF (eV)	k_{eff} versus EALF		Total uncertainty
				Bias	Fit uncertainty	
PWR SFP	2.59	10	0.202	-1.44×10^{-3}	6.82×10^{-3}	1.44×10^{-2}
	5.15	40	0.295	-1.32×10^{-3}	6.82×10^{-3}	1.44×10^{-2}
GBC-32	2.37	10	0.201	-1.44×10^{-3}	6.82×10^{-3}	1.44×10^{-2}
	4.9	40	0.295	-1.32×10^{-3}	6.82×10^{-3}	1.44×10^{-2}
BWR	5.0	11	0.456	-1.11×10^{-3}	6.82×10^{-3}	1.44×10^{-2}
Application model	**Initial enrichment (wt % ^{235}U)**	**Final BU (GWd/MTU)**	**Final enrichment (wt % ^{235}U)**	**k_{eff} vs. final enrichment**		**Total uncertainty**
				Bias	**Fit uncertainty**	
PWR SFP	2.59	10	1.956	-1.57×10^{-3}	6.81×10^{-3}	1.46×10^{-2}
	5.15	40	2.227	-1.55×10^{-3}	6.81×10^{-3}	1.46×10^{-2}
GBC-32	2.37	10	1.780	-1.58×10^{-3}	6.81×10^{-3}	1.46×10^{-2}
	4.9	40	2.150	-1.56×10^{-3}	6.81×10^{-3}	1.46×10^{-2}
BWR	5.0	11	3.820	-1.45×10^{-3}	6.81×10^{-3}	1.46×10^{-2}
Application model	**Initial enrichment (wt % ^{235}U)**	**Final BU (GWd/MTU)**	**Final Pu content (wt % Pu)**	**k_{eff} vs. final Pu content**		**Total uncertainty**
				Bias	**Fit uncertainty**	
PWR SFP	2.59	10	0.427	-2.05×10^{-3}	6.69×10^{-3}	1.42×10^{-2}
	5.15	40	1.212	-1.97×10^{-3}	6.69×10^{-3}	1.42×10^{-2}
GBC-32	2.37	10	0.416	-2.05×10^{-3}	6.69×10^{-3}	1.42×10^{-2}
	4.9	40	1.144	-1.97×10^{-3}	6.69×10^{-3}	1.42×10^{-2}
BWR	5.0	11	0.331	-2.06×10^{-3}	6.69×10^{-3}	1.42×10^{-2}

Table IV. Bias and bias uncertainty results using S/U analysis

Application model	Initial enrichment (wt % ^{235}U)	Final BU (GWd/MTU)	EALF (eV)	k_{eff} versus EALF		Total uncertainty
				Bias	Fit uncertainty	
PWR SFP	2.59	10	0.202	-1.75×10^{-3}	2.10×10^{-3}	7.2×10^{-3}
	5.15	40	0.295	-1.68×10^{-3}	3.46×10^{-3}	1.04×10^{-2}
GBC-32	2.37	10	0.201	-1.71×10^{-3}	1.92×10^{-3}	6.6×10^{-3}
	4.9	40	0.295	-2.45×10^{-3}	5.42×10^{-3}	1.30×10^{-2}
Application model	**Initial enrichment (wt % ^{235}U)**	**Final BU (GWd/MTU)**	**Final enrichment (wt % ^{235}U)**	**k_{eff} vs. final enrichment**		**Total uncertainty**
				Bias	**Fit uncertainty**	
PWR SFP	2.59	10	1.956	none	none	none
	5.15	40	2.227	none	none	none
GBC-32	2.37	10	1.780	none	none	none
	4.9	40	2.150	none	none	none
Application model	**Initial enrichment (wt % ^{235}U)**	**Final BU (GWd/MTU)**	**Final Pu content (wt % Pu)**	**k_{eff} vs. final Pu content**		**Total uncertainty**
				Bias	**Fit uncertainty**	
PWR SFP	2.59	10	0.427	none	none	none
	5.15	40	1.212	-2.03×10^{-3}	2.95×10^{-3}	9.5×10^{-3}
GBC-32	2.37	10	0.416	none	none	none
	4.9	40	1.144	-2.35×10^{-3}	4.76×10^{-3}	1.10×10^{-2}
Application model	**Initial enrichment (wt % ^{235}U)**	**Final BU (GWd/MTU)**	**Application c_k value**	**k_{eff} vs. c_k**		**Total uncertainty**
				Bias	**Fit uncertainty**	
PWR SFP	2.59	10	1	-6.12×10^{-3}	2.09×10^{-3}	1.07×10^{-2}
	5.15	40	1	3.08×10^{-3}	2.84×10^{-3}	8.9×10^{-3}
GBC-32	2.37	10	1	-4.03×10^{-3}	1.91×10^{-3}	7.47×10^{-3}
	4.9	40	1	1.92×10^{-3}	4.68×10^{-3}	1.08×10^{-2}

Table V. Uncertainty in k_{eff} due to uncertainty in nuclear data for BUC application models

	BUC model k_{eff} uncertainty (Δk)				
Model	**SFP**	**SFP**	**GBC-32**	**GBC-32**	**BWR**
Burnup (GWd/MTU)	**10**	**40**	**10**	**40**	**11**
All nuclides	0.00471	0.00486	0.00468	0.00545	0.00402
Major actinides (9)	0.00463	0.00476	0.00455	0.00527	0.00393
^{234}U	0.00000	0.00000	0.00000	0.00000	0.00000
^{235}U	0.00270	0.00211	0.00246	0.00226	0.00293
^{238}U	0.00250	0.00189	0.00246	0.00216	0.00211
^{238}Pu	0.00000	0.00003	0.00000	0.00003	0.00000
^{239}Pu	0.00281	0.00377	0.00292	0.00420	0.00154
^{240}Pu	0.00017	0.00042	0.00018	0.00046	0.00011
^{241}Pu	0.00008	0.00037	0.00007	0.00033	0.00003
^{242}Pu	0.00001	0.00013	0.00001	0.00014	0.00000
^{241}Am	0.00000	0.00002	0.00003	0.00018	0.00000
Minor actinides (3)	0.00007	0.00027	0.00007	0.00029	0.00013
^{243}Am	0.00000	0.00001	0.00000	0.00001	0.00000
^{237}Np	0.00002	0.00009	0.00002	0.00010	0.00001
^{236}U	0.00007	0.00025	0.00007	0.00027	0.00013
FP (16)	0.00022	0.00052	0.00024	0.00058	0.00023
^{95}Mo	0.00001	0.00004	0.00001	0.00006	0.00002
^{99}Tc	0.00002	0.00007	0.00002	0.00008	0.00003
^{101}Ru	0.00002	0.00008	0.00002	0.00008	0.00003
^{103}Rh	0.00004	0.00019	0.00006	0.00022	0.00008
^{109}Ag	0.00000	0.00002	0.00000	0.00002	0.00000
^{133}Cs	0.00005	0.00016	0.00005	0.00018	0.00008
^{147}Sm	0.00000	0.00002	0.00002	0.00006	0.00000
^{149}Sm	0.00015	0.00018	0.00016	0.00022	0.00010
^{150}Sm	0.00001	0.00005	0.00001	0.00006	0.00002
^{151}Sm	0.00008	0.00013	0.00008	0.00013	0.00006
^{152}Sm	0.00002	0.00006	0.00002	0.00007	0.00003
^{143}Nd	0.00011	0.00033	0.00012	0.00036	0.00014
^{145}Nd	0.00004	0.00017	0.00004	0.00018	0.00008
^{151}Eu	0.00000	0.00000	0.00000	0.00000	0.00000
^{153}Eu	0.00001	0.00007	0.00001	0.00008	0.00002
^{155}Gd	0.00000	0.00000	0.00001	0.00004	[a]
Other actinides	0.00003	0.00003	0.00000	0.00001	0.00000
Other FP	0.00015	0.00034	0.00008	0.00027	0.00014
Structural materials	0.00081	0.00073	0.00106	0.00118	0.00080

[a] ^{155}Gd is included in structural materials because it is not possible to distinguish between Gd added during manufacture and fission product ^{155}Gd.

Table VI. Bias and bias uncertainty from fission product experiments

Fission product[a]	Nuclear Data Uncertainty (Δk)[b]	Bias Value and Total Uncertainty (Δk) for Each Trending Parameter				
		EALF	Leakage Fraction	Mean Free Path	Water Level	Number of Fuel Rods
^{103}Rh (10)	4×10^{-5}	-2.0×10^{-5} $\pm 1.6\times10^{-4}$[c]	-2.1×10^{-4} $\pm 1.6\times10^{-4}$	-5.0×10^{-5} $\pm 1.6\times10^{-4}$	-1.1×10^{-4} $\pm 1.6\times10^{-4}$	-6.0×10^{-5} $\pm 1.6\times10^{-4}$
^{103}Rh (40)	1.9×10^{-4}	-6.0×10^{-5} $\pm 6.4\times10^{-4}$	-8.2×10^{-4} $\pm 6.4\times10^{-4}$	-2.2×10^{-4} $\pm 6.5\times10^{-4}$	-4.4×10^{-4} $\pm 6.5\times10^{-4}$	-2.4×10^{-4} $\pm 6.5\times10^{-4}$
^{133}Cs (10)	5×10^{-5}	5.0×10^{-5} $\pm 1.9\times10^{-4}$	-2.0×10^{-4} $\pm 1.9\times10^{-4}$	3.0×10^{-5} $\pm 1.9\times10^{-4}$	-2.0×10^{-5} $\pm 1.9\times10^{-4}$	3.0×10^{-5} $\pm 1.9\times10^{-4}$
^{133}Cs (40)	1.6×10^{-4}	1.5×10^{-4} $\pm 6.1\times10^{-4}$	-6.5×10^{-4} $\pm 6.1\times10^{-4}$	9.0×10^{-5} $\pm 6.1\times10^{-4}$	-5.0×10^{-5} $\pm 6.1x10^{-4}$	8.0×10^{-5} $\pm 6.1\times10^{-4}$
^{149}Sm (10)	1.5×10^{-4}	6.6×10^{-4} $\pm 7.7\times10^{-4}$	-1.1×10^{-4} $\pm 7.7\times10^{-4}$	5.0×10^{-4} $\pm 7.7\times10^{-4}$	1.3×10^{-4} $\pm 7.7\times10^{-4}$	4.3×10^{-4} $\pm 7.7\times10^{-4}$
^{149}Sm (40)	1.8×10^{-4}	8.4×10^{-4} $\pm 9.8\times10^{-4}$	-1.4×10^{-4} $\pm 9.8\times10^{-4}$	6.3×10^{-4} $\pm 9.8\times10^{-4}$	1.7×10^{-4} $\pm 9.8\times10^{-4}$	5.4×10^{-4} $\pm 9.8\times10^{-4}$
^{152}Sm (10)	2×10^{-5}	3.0×10^{-5} $\pm 1.3\times10^{-4}$	-1.1×10^{-4} $\pm 1.3\times10^{-4}$	3.0×10^{-5} $\pm 1.3\times10^{-4}$	-2.0×10^{-5} $\pm 1.3\times10^{-4}$	4.0×10^{-5} $\pm 1.3\times10^{-4}$
^{152}Sm (40)	6×10^{-5}	9.0×10^{-5} $\pm 3.9\times10^{-4}$	-3.1×10^{-4} $\pm 3.9\times10^{-4}$	8.0×10^{-5} $\pm 3.9\times10^{-4}$	-6.0×10^{-5} $\pm 3.9\times10^{-4}$	1.0×10^{-4} $\pm 3.9\times10^{-4}$
^{155}Gd (10)	0.0×10^{-5}	0.0 $\pm$ 0.0	0.0 $\pm$ 0.0	0.0 $\pm$ 0.0	0.0 $\pm$ 0.0	0.0 $\pm$ 0.0
^{155}Gd (40)	0.0×10^{-5}	0.0 $\pm 1.0\times10^{-5}$	-1.0×10^{-5} $\pm 1.0\times10^{-5}$	0.0 $\pm 1.0\times10^{-5}$	0.0 $\pm 1.0\times10^{-5}$	0.0 $\pm 1.0\times10^{-5}$
^{143}Nd (10)	1.1×10^{-4}	2.6×10^{-4} $\pm 6.5\times10^{-4}$	-4.7×10^{-4} $\pm 6.5\times10^{-4}$	1.7×10^{-4} $\pm 6.4\times10^{-4}$	-1.4×10^{-4} $\pm 6.5\times10^{-4}$	6.0×10^{-5} $\pm 6.4\times10^{-4}$
^{143}Nd (40)	3.3×10^{-4}	7.6×10^{-4} $\pm 1.9\times10^{-3}$	-1.4×10^{-3} $\pm 1.9\times10^{-3}$	4.9×10^{-4} $\pm 1.9\times10^{-3}$	-4.2×10^{-4} $\pm 1.9\times10^{-3}$	1.8×10^{-4} $\pm 1.9\times10^{-3}$
^{145}Nd (10)	4×10^{-5}	2.8×10^{-4} $\pm 8.0\times10^{-4}$	-6.7×10^{-4} $\pm 8.0\times10^{-4}$	1.7×10^{-4} $\pm 8.0\times10^{-4}$	-1.5×10^{-4} $\pm 8.0\times10^{-4}$	9.0×10^{-5} $\pm 8.0\times10^{-4}$
^{145}Nd (40)	1.7×10^{-5}	8.8×10^{-4} $\pm 2.6\times10^{-3}$	-2.1×10^{-3} $\pm 2.6\times10^{-3}$	5.5×10^{-4} $\pm 2.6\times10^{-3}$	-4.8×10^{-4} $\pm 2.6\times10^{-3}$	3.0×10^{-4} $\pm 2.6\times10^{-3}$

[a]Value in parentheses corresponds to SFP application model burnup in GWd/MTU.

[b]One standard deviation uncertainty due to nuclear data uncertainty from Table V.

[c]Quantity following ± is the 1 standard deviation uncertainty in bias due to uncertainty in the fit and Monte Carlo uncertainties in in the individual calculations used.

Manuscript title: An Approach for Validating Actinide and Fission Product Burnup Credit Criticality Safety Analyses – Criticality (k_{eff}) Predictions
Authors: J. M. Scaglione, D. E. Mueller and J. C. Wagner
Figure 1

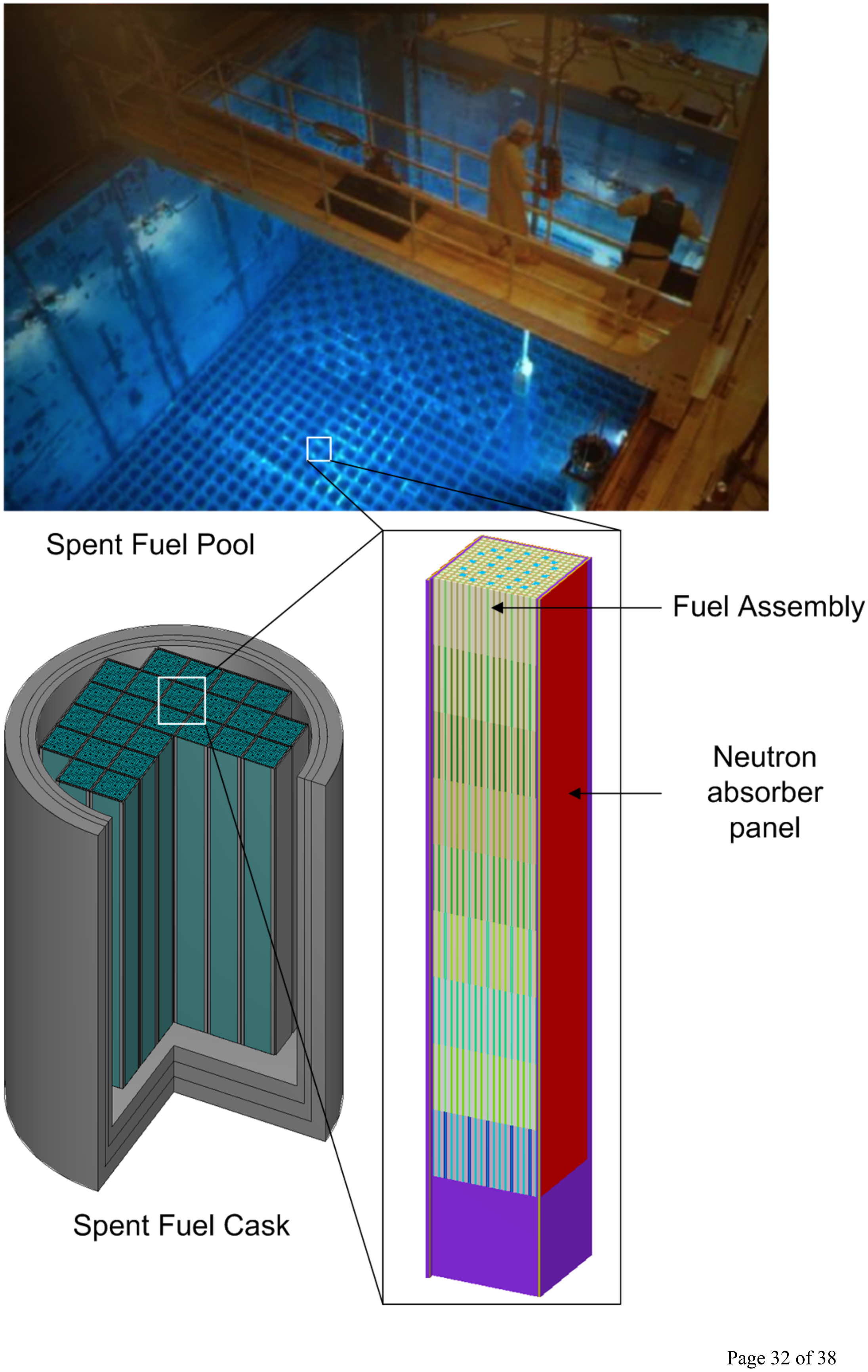

Manuscript title: An Approach for Validating Actinide and Fission Product Burnup Credit Criticality Safety Analyses – Criticality (k_{eff}) Predictions
Authors: J. M. Scaglione, D. E. Mueller and J. C. Wagner
Figure 2

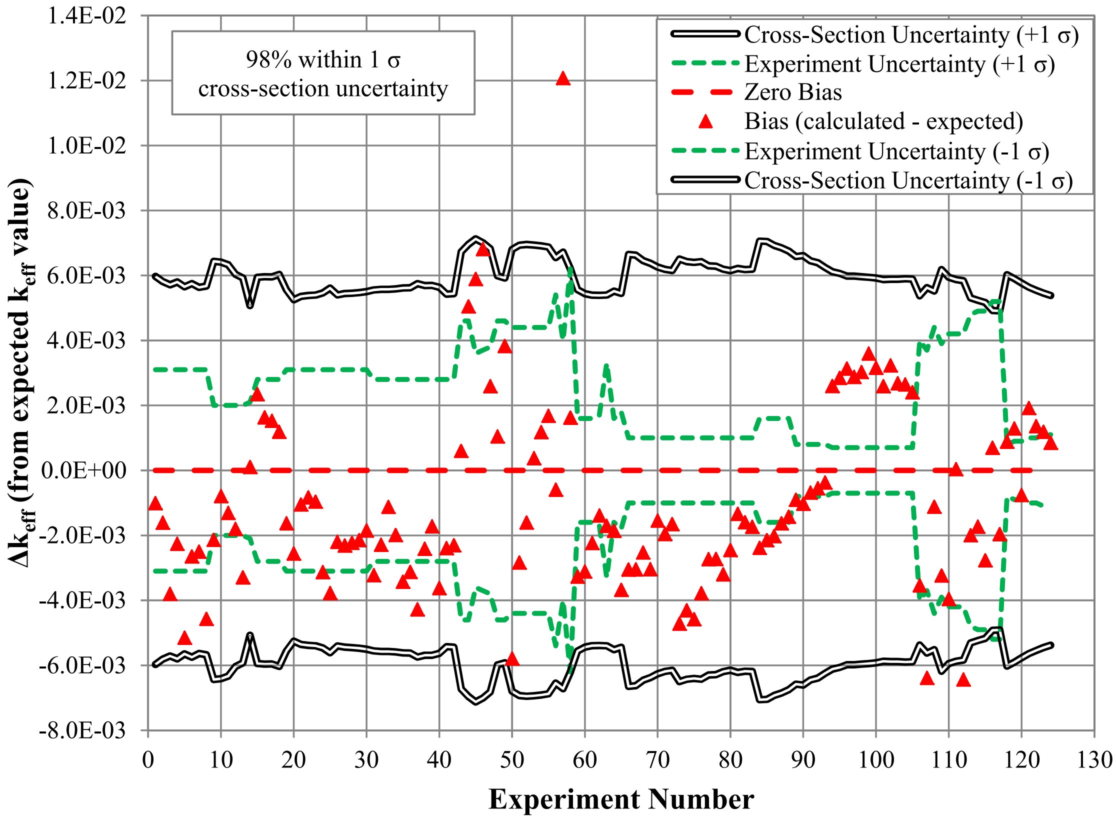

Manuscript title: An Approach for Validating Actinide and Fission Product Burnup Credit Criticality Safety Analyses – Criticality (k_{eff}) Predictions
Authors: J. M. Scaglione, D. E. Mueller and J. C. Wagner
Figure 3

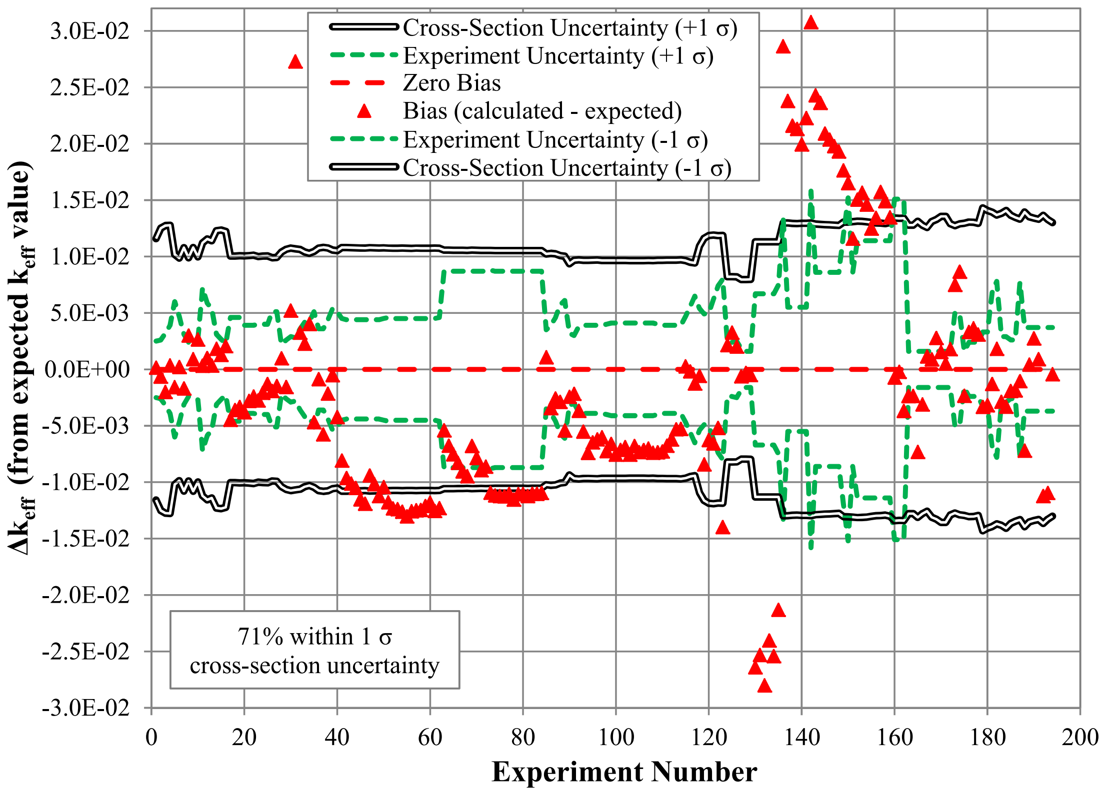

Manuscript title: An Approach for Validating Actinide and Fission Product Burnup Credit Criticality Safety Analyses – Criticality (k_{eff}) Predictions
Authors: J. M. Scaglione, D. E. Mueller and J. C. Wagner
Figure 4

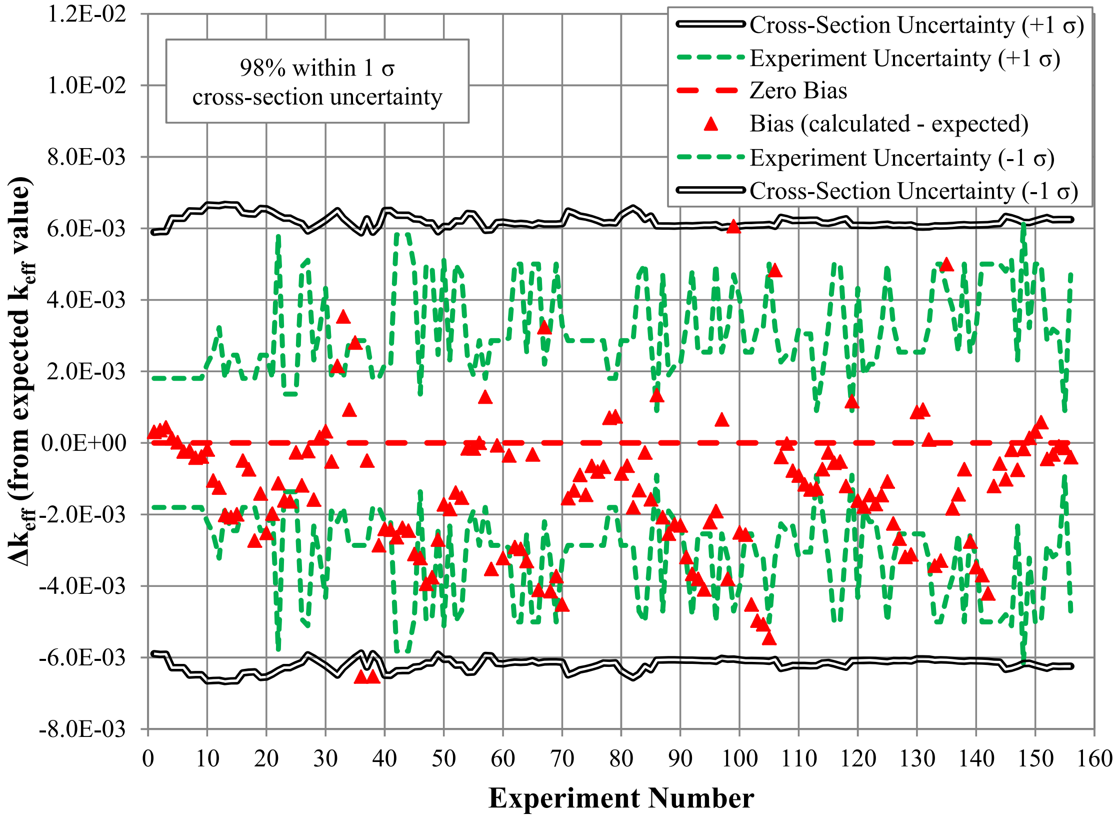

Manuscript title: An Approach for Validating Actinide and Fission Product Burnup Credit Criticality Safety Analyses – Criticality (k_{eff}) Predictions
Authors: J. M. Scaglione, D. E. Mueller and J. C. Wagner
Figure 5

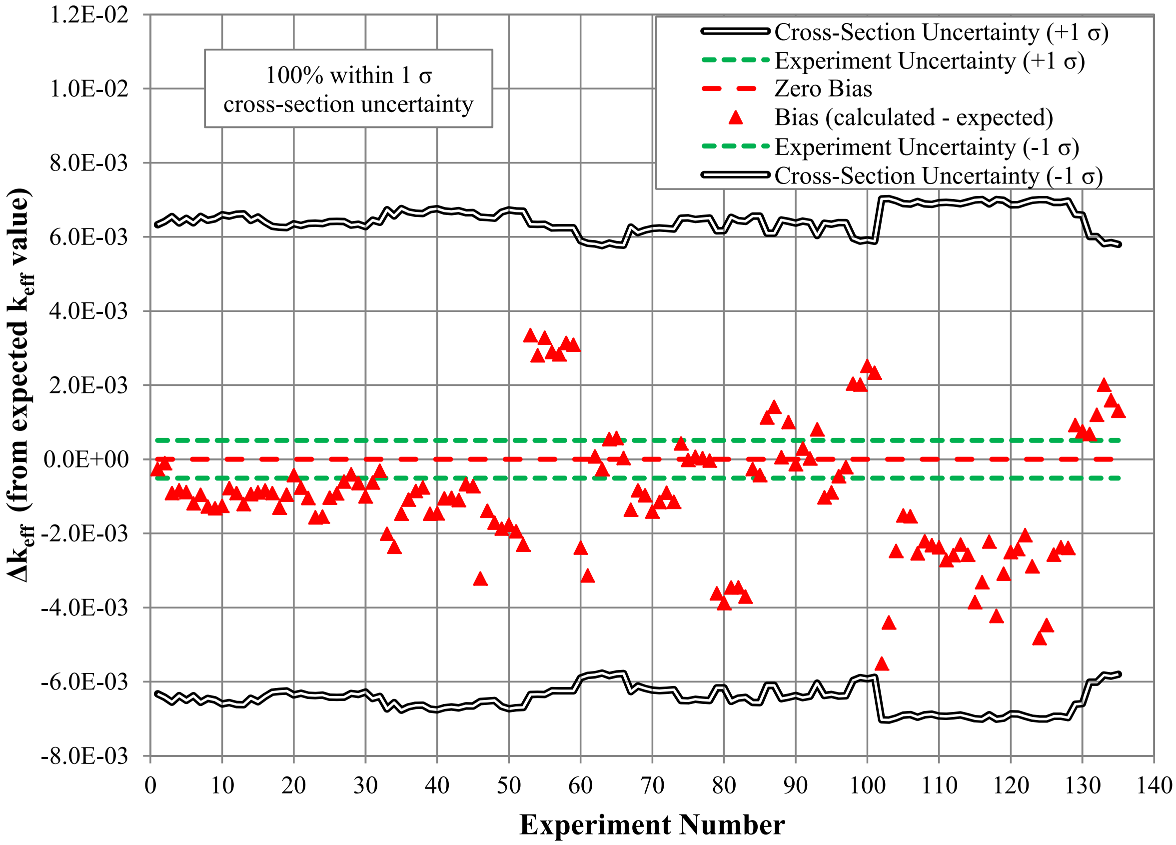

Figure 6

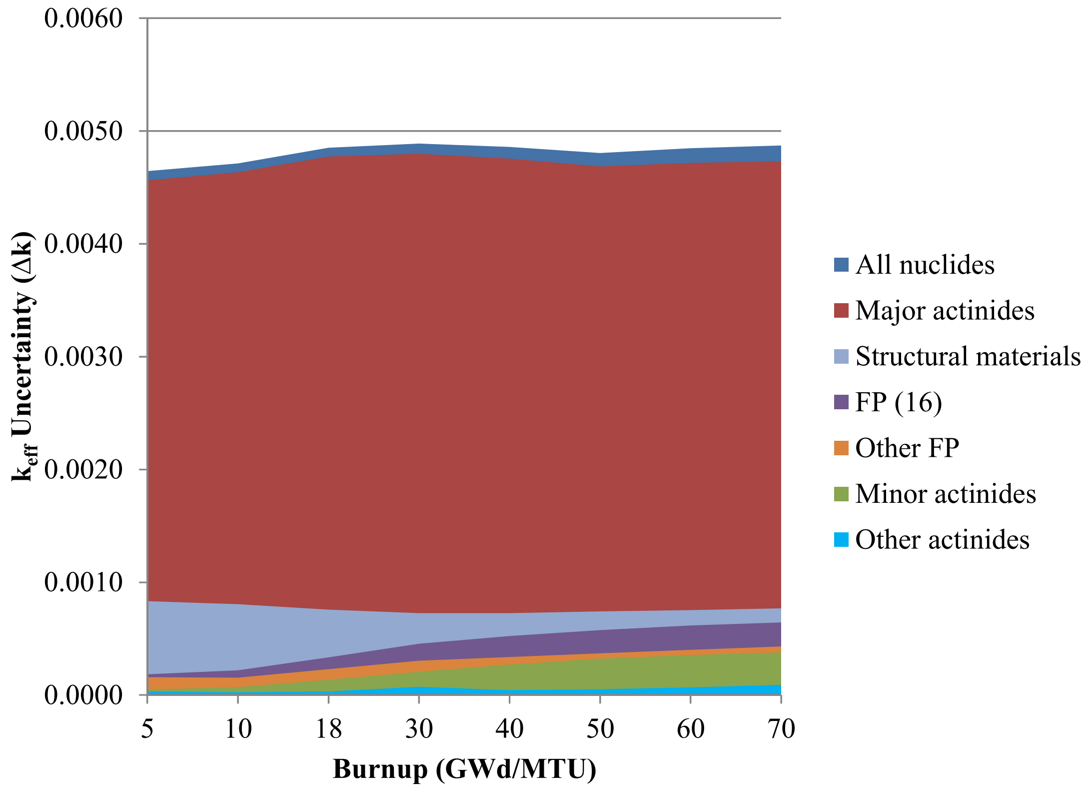
0.0060
0.0050
0.0040
0.0030
0.0020
0.0010
0.0000
keff Uncertainty (Δk)
5
10
18
30
40
50
60
70
Burnup (GWd/MTU)
All nuclides
Major actinides
Structural materials
FP (16)
Other FP
Minor actinides
Other actinides

FIGURE CAPTIONS

1. Representative PWR application models.
2. Comparison of calculated biases and experiment-specific nuclear data uncertainty in k_{eff} for LEU experiments.
3. Comparison of calculated biases and experiment-specific nuclear data uncertainty in k_{eff} for MOX (non-HTC) experiments.
4. Comparison of calculated biases and experiment-specific nuclear data uncertainty in k_{eff} for HTC experiments.
5. Comparison of calculated biases and experiment-specific nuclear data uncertainty in k_{eff} for Fission Product Programme experiments.
6. Comparison of contributors to k_{eff} uncertainty.